PCCP

Theoretical analysis of NMR shieldings in XSe and XTe (X = Si, Ge, Sn and Pb): the spin-rotation constant saga†

Taye Beyene Demissie

The nuclear spin-rotation (NSR) and absolute nuclear magnetic resonance (NMR) shielding tensors of the nuclei in the series of $X^{77}Se$ and $X^{125}Te$ (X = ^{29}Si, ^{73}Ge, ^{119}Sn and ^{207}Pb) are calculated using four-component relativistic density functional theory (DFT) and coupled-cluster singles-doubles with a perturbative triples correction (CCSD(T)). The results for the NSR constants are compared to available experimental data. The best theoretical estimates are obtained when relativistic corrections from DFT are added to the accurate non-relativistic CCSD(T) results. All the calculated NSR constants are in excellent agreement with the corresponding experimental values. Even though there are previously estimated absolute shielding constants and spans from experimental NSR tensors, new accurate values are reported following the same approach used to calculate the NSR constants in this study. The main reasons for the discrepancy between the previously reported NMR properties and the accurate results obtained in this study are also discussed.

1. Introduction

Until recently,[1–3] it has been assumed that the absolute nuclear magnetic resonance (NMR) shielding constant can be estimated indirectly from the nuclear spin-rotation (NSR) constant, an approach experimentalists have been using for many years. The assumption was that the electronic contribution to the NSR constant $C_{K,iso}^{el}$ could be directly related to the paramagnetic contribution to the absolute shielding constant $\sigma_{K,iso}^{para}$ and then added to a calculated diamagnetic contribution $\sigma_{K,iso}^{dia}$ [4–7] to estimate $\sigma_{K,iso}$, as shown for example in eqn (1) for diatomic molecules:

$$\sigma_{K,iso} = \sigma_{K,iso}^{dia} + \sigma_{K,iso}^{para} \approx \left(\sigma_K^{dia,FA} + \frac{10^9 m_p}{2 m_e g_K B_r} C_{K,iso}^{nuc} \right) + \left(\frac{10^9 m_p}{2 m_e g_K B_r} \right) C_{K,iso}^{el} \qquad (1)$$

where $\sigma_K^{dia,FA}$ is the NMR shielding constant of the free atom K (in ppm); m_p and m_e are the proton and electron masses, respectively; g_K is the nuclear g factor of the K'th nucleus; B_r ($\hbar/(4\pi I_\perp)$) is the molecular rotational constant (in MHz); $\hbar$ is the reduced Plank's constant; $I_\perp$ is the perpendicular component of the moment of inertia; $C_{K,iso}^{nuc}$ and $C_{K,iso}^{el}$ are nuclear and

Centre for Theoretical and Computational Chemistry, Department of Chemistry, UiT The Arctic University of Norway, N-9037 Tromsø, Norway.
E-mail: taye.b.demissie@uit.no
† Electronic supplementary information (ESI) available. See DOI: 10.1039/c5cp07025b

electronic contributions to the isotropic NSR constant (C_K, in kHz), respectively. Similarly, the span of the shielding tensor for a diatomic molecule (which is a measure of the asymmetry of the electron density surrounding the nucleus) has been approximated from the experimental NSR constant using eqn (2):

$$\Omega_K = \left| \sigma_{K,\perp} - \sigma_{K,\parallel} \right| \approx \frac{10^9 m_p}{2 m_e g_K B_r} C_{K,\perp} \qquad (2)$$

where $\sigma_{K,\parallel}$ and $\sigma_{K,\perp}$ (in ppm) being the components of the shielding tensor parallel and perpendicular to the molecular axis, respectively.

These approaches have shortcomings due to missing relativistic corrections.[1,3,8–12] Nevertheless, absolute shielding constants and spans for many nuclei have been reported using these approaches. As have already been noted,[3,10–12] the approach may give reasonable results only for very light nuclei (in a molecule composed of very light atoms) where relativistic effects are small (see for instance ref. 13–15 and references therein). The results for heavy nuclei estimated using eqn (1) and (2) are inaccurate due to the neglected relativistic corrections.[10–12,16] Besides the approaches discussed above, the most popular computational methodologies are also based on the Schrödinger equation where relativistic corrections are missing, which really are important for both the heavy atoms as well as light atoms in the vicinity of the heavy ones.[17,18]

The theoretical calculations of NMR properties of heavy nuclei are demanding because one has to use the full four-component relativistic Dirac–Kohn–Sham (DKS) Hamiltonian

(as implemented, for example, in the ReSpect[19] and DIRAC[20] program packages) and in some cases the two-component spin–orbit zeroth-order regular approximation (SO-ZORA) (as implemented in the Amsterdam density functional, ADF[21]) in order to obtain reasonable results. Approaches employing the relativistic Hamiltonian are currently based on density functional theory (DFT). Although DFT is a powerful and elegant method of calculation, it has shortcomings since approximations are required for the exchange–correlation energy functional. The lack of relativistic corrections in most of the currently available quantum chemical packages is also another limitation. One can reduce these shortcomings only by combining the relativistic corrections obtained from non-relativistic and four-component relativistic DFT calculations with those obtained from highly accurate non-relativistic coupled-cluster calculations. For instance, good agreement between the NSR constants obtained using this scheme and the experimental values for various molecules have been reported.[10–12,22,23]

In this paper, the NSR and NMR absolute shielding tensors of the monoselenides and monotellurides of silicon, germanium, tin and lead ($X^{77}Se$ and $X^{125}Te$ where X = ^{29}Si, ^{73}Ge, ^{119}Sn and ^{207}Pb) with the ambition that the results will be used for future benchmarking of theoretical methods. These molecules are also interesting since their bulk materials are narrow band-gap semiconductors used in opto-electronic and semiconductor applications[24–26] and hence the results presented in this study are useful for improving our understanding of their molecular properties. As such, attention was given to obtain good agreement between the gas-phase experimental and the calculated NSR tensors and thereby determine the absolute shielding tensors of all nuclei using the same computational approach. The full four-component relativistic and coupled-cluster singles-doubles with perturbative triples corrections (CCSD(T)) approaches were used to determine these highly accurate results. Experimental gas-phase studies showed that all molecules are closed-shell linear molecules with $^1\Sigma^+$ ground states. However, the CCSD(T) calculations in this study predicted closed-shell $^1\pi$ singlet ground states.

For all the molecules, experimental gas-phase NSR constants were reported by Grabow and co-workers.[27–30] Following the same approach as in previous studies,[11,12,16] the nonzero component (not the trace) of the NSR tensors are reported. In addition, the signs of the experimental NSR constants were changed either to (+) or (−) based on the signs of the calculated values in this work to be consistent with the sign convention used by Flygare.[7]

2. Computational details

The highly accurate non-relativistic coupled-cluster singles-doubles with perturbative triples corrections CCSD(T) results for the NSR and NMR absolute shielding tensors were obtained using the coupled-cluster analytic linear response methods, developed by Gauss and Stanton[31,32] and implemented in the CFOUR program package.[33] The code has been modified locally to include the

g factors for the heavy nuclei. Fully uncontracted double-ζ polarized Douglas–Kroll–Hess (denoted as unc-DZP-DKH) basis sets[34–36] were used in one set of calculations, and the uncontracted atomic natural orbital-relativistic correlation-consistent basis sets (denoted as unc-ANO-RCC)[37] were used in another set of calculations. It is important to note that the CCSD(T) calculations for the molecules involving heavy atoms are very expensive. For example CCSD(T)/unc-DZP-DKH for SnSe took a walltime of only 46 hours, whereas CCSD(T)/unc-ANO-RCC for the same molecule needed 1328 hours. The results obtained from these two basis sets do not show big differences (*vide infra*).

The four-component Dirac–Kohn–Sham (DKS) relativistic DFT results were obtained using a development version of the program package ReSpect[19] employing the BP86[38,39] and B3LYP[40–42] functionals. The modules using the restricted magnetic balance scheme[43,44] and the restricted kinetic balance scheme[45] were used for the NMR absolute shielding and NSR tensor calculations, respectively. DFT basis set dependence studies for both NMR absolute shielding and NSR tensors were performed using Dyall's relativistically optimized all-electron valence double-ζ (v2z);[46,47] core-valence double-ζ (cv2z);[46,47] valence triple-ζ (v3z);[47,48] core-valence triple-ζ (cv3z);[47,48] valence quadruple-ζ (v4z)[47] and core-valence quadruple-ζ (cv4z)[47] basis sets. The corresponding non-relativistic DFT results, used for the analysis of relativistic effects, were obtained using BP86 and B3LYP functionals and the cv4z basis sets.

The gauge-including atomic orbitals (GIAOs)[49,50] were employed to ensure origin independence for the absolute shielding constant calculations, while the common gauge-origin (CGO) approach[45] was used for the NSR constant calculations using the ReSpect program. It is important to note that rotational London orbitals (RLOs) facilitate the basis set convergence for the calculation of NSR constants. However, these have not yet been implemented in ReSpect and hence large uncontracted all-electron basis sets were used to determine the relativistic corrections to the NSR constants. The basis set convergence study (*vide infra*) also shows well-converged CGO results. Relativistic and non-relativistic shielding calculations using the CGO approach were also performed for the purpose of analysis.

The scalar relativistic effects in the four-component calculations of NMR absolute shielding and NSR constants were calculated following the procedures used in ref. 16, 51 and 52. The scalar relativistic corrections were calculated as differences between the results obtained from calculations performed by removing the spin–orbit (SO) effects and the corresponding non-relativistic results. Similarly, the SO contributions to the NMR absolute shielding and NSR tensors were calculated as differences between the full four-component results and those with SO effects removed.[16,51,52]

Calculations of NMR absolute shielding constants were also performed using the two-component spin–orbit zeroth-order-regular approximation (SO-ZORA)[53,54] using the Amsterdam Density Functional (ADF, version 2014.01) program package[21] employing the BP86 and B3LYP functionals together with the all-electron quadruple-ζ quadruple polarized (QZ4P) Slater-type basis sets optimized for ZORA computations.[55]

This journal is © the Owner Societies 2016

Phys. Chem. Chem. Phys., 2016, **18**, 3112–3123 | 3113

Experimental geometries were reported for different isotopes of all the molecules. However, for the purpose of consistence and direct comparison, the isotopically independent Born–Oppenheimer experimental equilibrium bond lengths (r_e^{BO}) of r_e(Si–Se) = 2.05828249 Å, r_e(Si–Te) = 2.27354785 Å, r_e(Ge–Se) = 2.13460287 Å, r_e(Ge–Te) = 2.34014248 Å, r_e(Sn–Se) = 2.32559945 Å, r_e(Sn–Te) = 2.52281737 Å, r_e(Pb–Se) = 2.402308 Å and r_e(Pb–Te) = 2.595065 Å were used for all calculations, all taken from the studies of Grabow and co-workers.[27–30] All nuclear g-factors are taken from ref. 56.

3. Results and discussion

3.1. Nuclear spin-rotation constants

The basis set dependence of the NSR constants of all nuclei in the X^{77}Se and X^{125}Te (X = ^{29}Si, ^{73}Ge, ^{119}Sn and ^{207}Pb) molecules are presented in Table 1. For all molecules, basis set dependence is found to be very small and converged results are obtained using cv3z basis sets. However, the larger cv4z basis set was used in all the other calculations to obtain accurate NSR constants. In the same table, the results obtained with the B3LYP functional and the cv4z basis set are also compared to the BP86 results. The largest difference between the BP86 and B3LYP results is for C(Pb) in PbSe (6%) and C(Pb) in PbTe (5%).

In Table 2, non-relativistic results from HF, CCSD(T) and DFT calculations together with the four-component relativistic DFT results are presented. As the atoms become heavier, the non-relativistic methods underestimate the magnitude of the NSR constants. This is most pronounced for the lead nuclei. For instance, C(Pb) in PbSe calculated using NR/BP86 and CCSD(T)/unc-DZP-DKH are respectively −21.565 kHz and −18.312 kHz, whereas that calculated using DKS/BP86 is −52.981 kHz (≈146% change with respect to NR/BP86). For the Se and Te nuclei, with the exception of C(Te) in SiTe and GeTe (which show a 9% change between NR/BP86 and DKS/BP86), such big changes are not observed. When we compare the HF and CCSD(T) results, we also see that HF overestimates the NSR constants compared to the other NR approaches. In other words, the CCSD(T) results always lie in the bottom line of all the HF results. From Table 2, one can also see that correlation effects [CCSD(T)-HF] are important. For instance, the correlation effect for

C(Ge) in GeTe is −0.509 kHz (a 30% change), whereas it is 0.417 kHz for C(Se) in PbSe (a 5% change), see Tables 2 and 3. The differences between the CCSD(T) results using the unc-DZP-DKH and unc-ANO-RCC basis sets show very small basis set dependence. However, considering the size of the basis sets, the CCSD(T) results obtained using the latter basis set should be more accurate.

The relativistic corrections obtained from the two DFT functionals are listed in Table 3. Large relativistic corrections to the NSR constants are observed for lead in PbSe and PbTe compared to the other molecules. For instance, the relativistic correction calculated using the BP86 functional contributes to 15% of the total NSR constant of Ge in GeTe, but 28% for C(Sn) in SnTe and 64% for C(Pb) in PbTe. The B3LYP calculated results also show similar trends for the relativistic effects. For the C(Sn) and C(Pb) NSR tensors in all molecules, relativistic effects are more important than electron correlation effects. For example, the electron correlation effect on C(Sn) in SnSe is −5.650 kHz, whereas the BP86 relativistic correction is 8.486 kHz (see Table 3).

The results listed in Table 3 also show that CCSD(T) gives NSR constants of Ge in GeSe and GeTe with an approximate errors of 6% and 9% compared to the corresponding experimental values, whereas the error increases to 22% and 29% for C(Sn) in SnSe and SnTe, respectively. For C(Pb) in PbSe and PbTe, CCSD(T) underestimates these results by approximately 61% and 60%, respectively, compared to the experimental values as well as the final NSR results determined by adding the relativistic corrections (ΔC(rel)), obtained from DFT calculations, to the CCSD(T) calculated values. These analyses show the importance of combining the CCSD(T) and four-component relativistic DFT methodologies to obtain reasonably good results that can be compared to experimental values. With the exception of C(Pb) in PbTe (which show an error of 13%), all the final calculated NSR constants are in quite good agreement with the corresponding gas-phase experimental NSR constants. The most impressive final results are those of tin and lead where the errors of these final results are significantly reduced compared to the errors of the results obtained from the pure CCSD(T) and DFT calculations, indicating that the scheme followed in this study is a powerful remedy for these kinds of calculations. We have previously also employed this scheme to determine

Table 1 Basis set dependence of the DKS spin-rotation constants (C, in kHz) of nuclei in XSe and XTe (X = Ge, Sn and Pb) molecules[a]

	GeSe		GeTe		SnSe		SnTe		PbSe		PbTe	
	Ge	Se	Ge	Te	Sn	Se	Sn	Te	Pb	Se	Pb	Te
v2z	2.624	−15.596	2.120	29.136	35.947	−11.116	27.496	18.952	−52.115	−9.064	−36.495	13.636
cv2z	2.676	−15.823	2.160	29.433	36.387	−11.255	27.886	19.142	−52.603	−9.152	−36.859	13.751
v3z	2.700	−15.763	2.190	29.317	36.878	−11.298	28.373	19.260	−52.883	−9.172	−37.111	13.812
cv3z	2.732	−15.913	2.211	29.484	37.073	−11.357	28.517	19.319	−52.946	−9.175	−37.166	13.809
v4z	2.711	−15.819	2.199	29.370	36.998	−11.341	28.493	19.325	−52.935	−9.191	−37.194	13.848
cv4z	2.734	−15.931	2.214	29.485	37.110	−11.380	28.575	19.356	−52.981	−9.193	−37.236	13.842
cv4z[b]	2.688	−15.652	2.165	29.015	36.238	−11.122	27.691	18.961	−51.286	−8.955	−35.790	13.511
cv4z[c]	2.799	−16.226	2.288	29.996	38.100	−11.593	29.484	19.582	−56.132	−9.453	−39.089	14.027

[a] Calculated using BP86 unless stated otherwise. [b] Calculated using PBE. [c] Calculated using B3LYP.

3114 | *Phys. Chem. Chem. Phys.*, 2016, **18**, 3112–3123

This journal is © the Owner Societies 2016

Table 2 Comparison of calculated values for the spin-rotation constants (C, in kHz) of nuclei in XSe and XTe (X = Si, Ge, Sn and Pb) molecules at different computational levels

		NR					DKS	
		HF[a]	BP86[b]	B3LYP[b]	CCSD(T)[a]	CCSD(T)[c]	BP86[b]	B3LYP[b]
SiSe	Si	11.156	10.440	10.799	9.155	9.571	10.709	11.045
	Se	−25.980	−26.771	−26.897	−25.191	−23.686	−27.813	−27.886
SiTe	Si	10.143	8.952	9.405	7.808	8.242	9.481	9.892
	Te	51.706	52.892	53.576	48.012	47.536	57.562	57.857
GeSe	Ge	2.716	2.477	2.543	2.198	2.223	2.734	2.799
	Se	−16.598	−15.219	−15.536	−14.834	−13.515	−15.931	−16.226
GeTe	Ge	2.191	1.918	1.996	1.682	1.724	2.214	2.288
	Te	29.388	27.111	27.865	25.210	24.420	29.485	29.996
SnSe	Sn	30.811	28.624	29.360	25.161	25.718	37.110	38.100
	Se	−11.397	−10.796	−11.017	−10.597	−9.608	−11.380	−11.593
SnTe	Sn	23.006	20.890	21.630	18.189	19.942	28.575	29.484
	Te	18.493	18.025	18.453	16.889	15.831	19.356	19.582
PbSe	Pb	−23.104	−21.565	−22.082	−18.312	−17.996	−52.981	−56.132
	Se	−9.246	−8.645	−8.829	−8.526	−8.058	−9.193	−9.453
PbTe	Pb	−15.972	−14.787	−15.259	−12.440	—	−37.236	−39.089
	Te	13.849	13.517	13.830	12.681	—	13.842	14.027

[a] The unc-DZP-DKH basis set was used. [b] The Dyall-cv4z basis set was used. [c] The unc-ANO-RCC basis set was used; not calculated for PbTe due to a large number of electrons.

Table 3 Relativisitc corrections, estimated correlation effects, and final calculated values for the NSR constants (C, in kHz) of nuclei in XSe and XTe (X = Si, Ge, Sn and Pb) molecules together with the experimental values

		Δ(correl)[a]	ΔC(rel 1)[b]	ΔC(rel 2)[c]	CCSD(T)[d]	Total 1[e]	Total 2[f]	Exp.[g]
SiSe	Si	−2.001	0.269	0.246	9.571	9.840	9.817	(+)10.20[h]
	Se	0.789	−1.042	−0.989	−23.686	−24.728	−24.675	(−)25.46[h]
SiTe	Si	−2.335	0.529	0.487	8.242	8.771	8.729	(+)9.22[h]
	Te	−3.694	4.670	4.281	47.536	52.206	51.817	(+)53.75[h]
GeSe	Ge	−0.518	0.257	0.256	2.223	2.480	2.479	(+)2.330(27)[i]
	Se	1.764	−0.712	−0.690	−13.515	−14.227	−14.205	(−)13.70(19)[i]
GeTe	Ge	−0.509	0.296	0.292	1.724	2.020	2.016	(+)1.847(45)[i]
	Te	−4.178	2.374	2.131	24.420	26.794	26.551	(+)26.130(97)[i]
SnSe	Sn	−5.650	8.486	8.740	25.718	34.204	34.458	(+)32.34(83)[j]
	Se	0.800	−0.584	−0.576	−9.608	−10.192	−10.184	(−)10.11(82)[j]
SnTe	Sn	−4.817	7.685	7.854	19.942	27.627	27.796	(+)25.48(17)[j]
	Te	−1.604	1.331	1.129	15.831	17.162	16.960	(+)16.53(16)[j]
PbSe	Pb	4.792	−31.416	−34.050	−17.996	−49.412	−52.046	(−)47.04(32)[k]
	Se	0.417	−0.548	−0.624	−8.058	−8.606	−8.682	(−)9.35(23)[k]
PbTe	Pb	3.532	−22.449	−23.830	−12.440	−34.889	−36.270	(−)30.91(44)[k]
	Te	−1.168	0.325	0.510	12.681	13.006	13.191	(+)13.58(44)[k]

[a] Δ(correl) is an estimated electron correlation effect [CCSD(T)-HF] (see Table 2). [b] ΔC(rel 1) is the difference between DKS and NR results using BP86/cv4z (see Table 2). [c] ΔC(rel 2) is the difference between DKS and NR results using B3LYP/cv4z (see Table 2). [d] unc-ANO-RCC (unc-DZP-DKH for PbTe) basis sets (see Table 2). [e] Total 1 is the sum of ΔC(rel 1) and the CCSD(T) calculated values. [f] Total 2 is the sum of ΔC(rel 2) and the CCSD(T) calculated values. [g] Experimental values for different isotopes are given in the corresponding references. [h] Taken from ref. 27. [i] Taken from ref. 28. [j] Taken from ref. 29. [k] Taken from ref. 30.

Table 4 Basis set dependence of the DKS absolute shielding constants (σ, in ppm) of nuclei in XSe and XTe (X = Ge, Sn and Pb) molecules[a]

	GeSe		GeTe		SnSe		SnTe		PbSe		PbTe	
	Ge	Se	Ge	Te	Sn	Se	Sn	Te	Pb	Se	Pb	Te
v2z	181.0	207.0	−356.5	1516.9	857.9	−14.3	−47.5	1424.6	−264.2	−209.4	−2496.1	1509.7
cv2z	168.3	198.5	−379.3	1503.7	833.3	−26.5	−91.7	1408.0	−398.2	−227.0	−2637.8	1492.6
v3z	111.9	205.2	−449.1	1483.7	717.4	−1.6	−228.9	1405.5	−659.0	−163.5	−2900.3	1550.0
cv3z	110.2	204.9	−455.6	1485.1	722.0	1.4	−232.8	1410.2	−637.2	−158.8	−2897.1	1556.0
v4z	107.2	204.8	−456.8	1479.8	704.8	1.2	−249.4	1404.2	−701.7	−152.9	−2968.9	1557.1
cv4z	107.8	207.5	−457.9	1485.6	715.7	8.9	−241.4	1415.7	−672.5	−147.7	−2943.3	1564.3
cv4z[b]	104.0	212.5	−456.8	1499.1	705.2	31.0	−252.3	1450.8	−770.0	−119.5	−3077.0	1601.2

[a] Calculated using BP86 employing the GIAO approach unless stated otherwise. [b] Calculated using BP86 employing the CGO approach.

the NSR constants of 47 nuclei in 22 molecules.[10–12,16,22] All these studies point to the need for relativistic coupled-cluster methods for the calculation of magnetic properties.

3.2. NMR shielding constants

A basis set dependence study of the absolute shielding constants are presented in Table 4. For all nuclei, with the exception of σ(Te), there are considerable differences between the double-ζ results and those obtained using other basis sets. As the size of the basis sets increase, the results become more stable showing convergence to the basis set limit. Hence, the larger cv4z basis set was used for the remaining calculations of the absolute shielding tensors. This is important especially for the results calculated using B3LYP employing the CGO approach. Similarly, the all-electron QZ4P basis set was also used for the calculations performed in ADF.

The absolute shielding constants obtained using different methods are listed in Table 5. Comparing the NR results obtained from both the coupled-cluster and DFT calculations shows that none of the NR methods give close results among each other for most of the molecules. The results obtained using the BP86 and B3LYP functionals show that the dependence of σ(Te) in all molecules is small compared to the other nuclei, whereas considerable dependence on the functional as well as the Hamiltonian is observed for the other nuclei. This dependence is most pronounced for σ(Pb). For example, σ(Sn) in SnTe calculated using DKS/BP86 −241.4 ppm and using DKS/B3LYP is −486.8 ppm, and σ(Pb) in PbTe using DKS/BP86 is −2943.3 ppm and using DKS/B3LYP is −4173.0 ppm. Test calculations for these two nuclei using DKS/PBE also show considerable differences from the above results. One may suspect slower basis set convergence (since the B3LYP results are obtained employing CGOs), however, the results listed in Table 4 (compare the last two rows) show that the results

obtained employing the CGO and GIAO approaches do not show big differences. Moreover, additional calculations using DKS/B3LYP were also performed by putting the gauge-origin on tin and lead atoms. The results obtained in this case for Pb in both PbSe and PbTe do not show considerable differences, for instance σ(Pb) and σ(Te) in PbTe when the gauge-origin is on Pb are −4171.1 and 1474.5 ppm, respectively (to be compared with −4173.0 and 1491.8 ppm, respectively, when the gauge-origin is at the center of mass). Similarly, σ(Sn) and σ(Te) in SnTe calculated by putting the gauge on Sn are −473.3 and 1390.3 ppm, whereas those calculated by putting the gauge-origin at the center of mass are −486.8 and 1399.2 ppm, respectively.

The two- and four-component results listed in Table 5 show that the two Hamiltonians give very different results, especially for the heavier atoms. For instance, σ(Te) in SnTe using SO-ZORA/BP86 is 857.8 ppm and using SO-ZORA/B3LYP is 894.5 ppm, whereas those calculated using DKS/BP86 and DKS/B3LYP are 1415.7 ppm and 1399.2 ppm, respectively. It is important to note that one may improve (but not always) the SO-ZORA results by introducing dispersion correction[57] to the functional. For instance, σ(Sn) and σ(Te) calculated using SO-ZORA/BP86-D3/QZ4P are −283.9 ppm and 757.5 ppm, respectively. If we take the DKS/BP86 results as benchmarks, we see that the former shows improvement and that of Te gets worse compared to those obtained using SO-ZORA/BP86.

In Table 6, the paramagnetic and diamagnetic contributions to the shielding tensors are presented together with the corresponding values of the paramagnetic contributions determined from the electronic contribution to the NSR tensors. From the results we see that the paramagnetic contribution to all nuclear shielding tensors obtained from the direct calculations of the absolute shielding tensors are the same as to those derived from the electronic contribution to the NSR tensors in the non-relativistic theory. For example, $C^{\mathrm{el,iso}}$(Pb) in PbTe calculated

Table 5 Comparison of calculated values for the absolute shielding constants (σ, in ppm) of nuclei in XSe and XTe (X = Si, Ge, Sn and Pb) molecules at different computational levels

		NR					SO-ZORA		DKS	
		HF[a]	BP86[b]	B3LYP[c]	CCSD(T)[a]	CCSD(T)[d]	BP86[e]	B3LYP[e]	BP86[b]	B3LYP[c]
SiSe	Si	−211.4	−140.8	−175.9	−16.1	−56.9	−144.7	−181.1	−149.8	−183.1
	Se	377.3	297.6	284.8	456.6	608.5	341.0	371.5	481.7	474.5
SiTe	Si	−471.5	−312.5	−372.8	−161.1	−218.9	−346.5	−412.9	−371.9	−423.0
	Te	1078.3	980.4	923.4	1384.1	1423.8	1178.1	1324.2	1798.1	1778.9
GeSe	Ge	−114.4	139.2	69.0	433.1	407.3	75.4	−10.8	107.8	33.4
	Se	−205.0	61.4	0.1	135.3	389.8	90.0	45.2	207.5	155.8
GeTe	Ge	−666.6	−239.4	−361.3	129.0	63.5	−421.2	−583.1	−457.9	−582.4
	Te	312.5	704.1	574.3	1030.2	1166.2	967.4	956.8	1485.6	1420.0
SnSe	Sn	584.7	905.2	797.3	1410.2	1328.9	579.4	364.6	715.8	553.3
	Se	−258.7	−87.0	−150.3	−30.3	252.3	−122.4	−164.9	8.9	−30.9
SnTe	Sn	−72.4	403.0	236.7	1007.5	966.4	−196.7	−549.6	−241.4	−486.8
	Te	476.3	600.4	486.9	899.9	930.7	857.8	894.5	1415.7	1399.2
PbSe	Pb	2419.3	2927.4	2756.3	4004.3	3876.7	142.6	−1389.0	−672.5	−1862.1
	Se	−387.1	−167.0	−234.4	−123.5	−196.9	−260.4	246.0	−147.7	−240.9
PbTe	Pb	1497.9	2133.0	1879.1	3392.0	—	−1206.2	−3034.5	−2943.3	−4173.0
	Te	411.5	530.6	418.3	828.8	—	981.4	1048.7	1564.3	1491.8

[a] The unc-DZP-DKH basis set was used. [b] The Dyall-cv4z basis set was used together with the GIAO approach. [c] The Dyall-cv4z basis set was used together with the CGO approach. [d] The unc-ANO-RCC basis set was used; not calculated for PbTe due to a large number of electrons. [e] The all-electron QZ4P basis set was used together with the GIAO approach.

3116 | *Phys. Chem. Chem. Phys.*, 2016, **18**, 3112–3123

This journal is © the Owner Societies 2016

Table 6 Comparison of the calculated electronic contributions to C, paramagnetic contributions to σ, diamagnetic contributions to σ, shielding spans (Ω) and the perpendicular component of the isotropic C for nuclei in XSe and XTe (X = Si, Ge, Sn and Pb) (all in ppm). All calculated using BP86/cv4z employing the CGO approach for all calculations

	NR[a]	DKS[b]	Previous[c]	NR[a]	DKS[b]	Previous[c]
SiSe	**Si**			**Se**		
$C^{\mathrm{el,iso}}$	−1057.7	−1083.8	−1147.0[d]	−2748.1	−2853.2	−2644.9[d]
$\sigma^{\mathrm{para,iso}}$	−1057.7	−1067.6	−1167[d]	−2748.1	−2582.4	−2573[d]
$\sigma^{\mathrm{dia,iso}}$	916.9	917.7	1061[e]	3045.7	3064.2	3362[e]
Ω	1535.8	1605.0	1518[d]	4064.0	4284.1	3764[d]
$C_{\perp}$	−1522.8	−1562.0	−1487.8[d]	−4052.6	−4210.2	−3854.1[d]
SiTe	**Si**			**Te**		
$C^{\mathrm{el,iso}}$	−1227.4	−1297.4	−1435.1[d]	−4429.7	−4816.6	−4511.5[d]
$\sigma^{\mathrm{para,iso}}$	−1227.4	−1281.6	−1445[d]	−4429.7	−3692.1	−4394[d]
$\sigma^{\mathrm{dia,iso}}$	914.9	915.6	1121[e]	5410.0	5487.8	6623[e]
Ω	1796.5	1996.3	1845[d]	6582.8	7404.1	6505[d]
$C_{\perp}$	−1780.3	−1885.4	−1833.6[d]	−6574.1	−7154.5	−6680.7[d]
GeSe	**Ge**			**Se**		
$C^{\mathrm{el,iso}}$	−2690.6	−2962.9	−2608.7[f]	−3010.3	−3147.8	−2783.3[f]
$\sigma^{\mathrm{para,iso}}$	−2690.6	−2740.5	−2662[f]	−3010.3	−2877.4	−2808[f]
$\sigma^{\mathrm{dia,iso}}$	2829.8	2844.5	3134[e]	3071.6	3089.9	3439[e]
Ω	3938.4	4482.9	3768[f]	4421.4	4743.5	4001[f]
$C_{\perp}$	−3926.6	−4335.2	−3694[f]	−4406.9	−4613.2	−3967[f]
GeTe	**Ge**			**Te**		
$C^{\mathrm{el,iso}}$	−3073.3	−3536.9	−3090.7[f]	−4740.1	−5147.9	−4669.3[f]
$\sigma^{\mathrm{para,iso}}$	−3073.3	−3305.3	−3140[f]	−4740.1	−4022.7	−4635.3[f]
$\sigma^{\mathrm{dia,iso}}$	2833.9	2848.5	3194[e]	5444.2	5521.8	6693[e]
Ω	4509.5	5531.3	4397[f]	6999.7	7948.1	6760[f]
$C_{\perp}$	−4494.4	−5189.8	−4329[f]	−6988.6	−7600.4	−6811[f]
SnSe	**Sn**			**Se**		
$C^{\mathrm{el,iso}}$	−4264.0	−5503.4	−4800.7[g]	−3165.8	−3332.7	−3304.7[g]
$\sigma^{\mathrm{para,iso}}$	−4264.0	−4531.6	−4912[g]	−3165.8	−3065.9	−3317.3[g]
$\sigma^{\mathrm{dia,iso}}$	5169.2	5236.8	6203[e]	3078.9	3096.9	3327[e]
Ω	6279.6	8695.6	7163[g]	4647.4	5165.3	4672[g]
$C_{\perp}$	−6271.0	−8130.2	−7000[g]	−4629.7	−4880.0	−4674[g]
SnTe	**Sn**			**Te**		
$C^{\mathrm{el,iso}}$	−4777.3	−6499.9	−5167.3[g]	−4858.2	−5209.9	−4869.3[g]
$\sigma^{\mathrm{para,iso}}$	−4777.3	−5499.8	−5263.3[g]	−4858.2	−4085.1	−4886[g]
$\sigma^{\mathrm{dia,iso}}$	5180.2	5247.5	6203[e]	5458.6	5535.9	6639[e]
Ω	7036.0	10670.4	7604[g]	7158.3	8282.9	7049[g]
$C_{\perp}$	−7024.3	−9608.4	−7461[g]	−7144.3	−7672.0	−7020[g]
PbSe	**Pb**			**Se**		
$C^{\mathrm{el,iso}}$	−7228.8	−17618.0	15620.7[h]	−3253.5	−3454.2	3747.33[h]
$\sigma^{\mathrm{para,iso}}$	−7228.8	−11297.0	−15976[h]	−3253.5	−3223.4	−3749.3[h]
$\sigma^{\mathrm{dia,iso}}$	10156.2	10527.0	20688[e]	3086.5	3104.0	3619[e]
Ω	10705.4	31678.3	23765[h]	4770.4	6130.5	5143[h]
$C_{\perp}$	−10697.9	−26282.0	23335[h]	−4749.8	−5051.0	5137[h]
PbTe	**Pb**			**Te**		
$C^{\mathrm{el,iso}}$	−8043.7	−20078.0	16778.7[h]	−4944.5	−5060.7	5156[h]
$\sigma^{\mathrm{para,iso}}$	−8043.7	−13624.0	−17059[h]	−4944.5	−3950.3	−5157.3[h]
$\sigma^{\mathrm{dia,iso}}$	10176.6	10546.8	20743[e]	5475.0	5551.5	6862[e]
Ω	11900.0	37812.2	25306[h]	7265.6	9319.6	7172[h]
$C_{\perp}$	−11889.4	−29941.0	24854[h]	−7249.2	−7423.5	7283[h]

[a] NR stands for non-relativistically calculated results using BP86/cv4z. [b] DKS stands for full four-component relativistically calculated results using BP86/cv4z. [c] $C^{\mathrm{el,iso}}$ and $C_{\perp}$ are converted (kHz to ppm) values, $\sigma^{\mathrm{para,iso}}$ is estimated from $C^{\mathrm{el,iso}}$ and Ω is estimated from $C_{\perp}$. [d] Taken from ref. 27. [e] Calculated diamagnetic contribution reported in the corresponding references. [f] Taken from ref. 28. [g] Taken from ref. 29. [h] Taken from ref. 30.

using NR/BP86 is −8043.7 ppm, and $\sigma^{\mathrm{para,iso}}$(Pb) in the same molecule obtained using NR/BP86 is −8043.7 ppm. This is because the magnetic and angular momentum operators have the same form in the non-relativistic theory.[1,2] On the other hand, there is no agreement between $C^{\mathrm{el,iso}}$ and $\sigma^{\mathrm{para,iso}}$ in the

four-component relativistic calculations. In the four-component relativistic theory, the magnetic and angular momentum operators are different since the magnetic momentum operator couples the large and small components of the wave function, whereas the total angular momentum operator does not.[1,2,16] This makes

This journal is © the Owner Societies 2016

Phys. Chem. Chem. Phys., 2016, **18**, 3112–3123 | **3117**

the paramagnetic contribution obtained from the four-component relativistic calculations to be different from the one derived from the electronic contribution to the NSR tensors. The difference becomes large as the nuclei become heavier. For instance, the values of $C^{el,iso}$(Ge) and $\sigma^{para,iso}$(Ge) in GeSe calculated using DKS/BP86 are -2962.9 ppm and -2740.5 ppm, respectively (a difference of 222.4 ppm), but for Pb in PbTe these values are -20078.0 ppm and -13624.0 ppm, respectively (a difference of 6454 ppm).

The correlations between the paramagnetic contributions from direct calculations of the absolute shielding tensors and the electronic contributions to the NSR tensors are shown in Fig. 1. Surprisingly, the trends show a periodic behavior. For example, the difference between $C^{el,iso}$ and $\sigma^{para,iso}$ of Ge and Se (which are both in period 4 of the periodic table) in all the molecules lie within the 222–270 ppm range. Similarly, these differences for Sn and Te (both in period 5) are within a range of 972–1125 ppm (see Table 6 and Fig. 1 for details). Additional test calculations were also done for SnPo and PbPo. The results show that these differences for Pb and Po lie within the range of 6320–7500 ppm. From Fig. 1, one can also see that the differences between $C^{el,iso}$ and $\sigma^{para,iso}$ (also they refer to the relativistic corrections to the shielding tensor) are atomic in nature. For instance, the difference between $C^{el,iso}$ and $\sigma^{para,iso}$ of Te in all molecules is 1125 ppm (1110 ppm in PbTe), indicating that the difference is independent of the nature of the atom bonded to tellurium. These differences also indicate that the absolute shielding scales determined indirectly from experimental NSR constants are off by the above numbers for

the respective nuclei, keeping in mind that the diamagnetic contributions are obtained using appropriate shielding calculations. Further studies using perturbation analysis are underway in our group to investigate the validity of these differences.[58]

The relativistic corrections, electron correlation effects and final calculated absolute shielding constants are presented in Table 7, together with the previously determined values from experimental NSR tensors. The relativistic correction, the differences between the DKS and NR results, that is obtained from both functionals increase as the atoms become heavier. The effect of the heavy atom on the neighboring nucleus can also be seen from Table 7. For instance, the relativistic correction for σ(Sn) in SnSe calculated using BP86 is -189.4 ppm, whereas that in SnTe is -644.4 ppm. Similarly, the relativistic correction calculated using BP86 for σ(Te) is 781.5 ppm in GeTe, 815.3 ppm in SnTe and 1033.7 ppm in PbTe, showing the effect of the neighboring atoms on the absolute shielding constant of tellurium.

With the exception of the nuclei in PbSe and PbTe, the final absolute shielding constants obtained by adding the CCSD(T) calculated results to the $\Delta\sigma$(rel) values obtained from BP86 and B3LYP are in good agreement with each other (see Table 7). On the other hand, with the exception of a very few nuclei, the previously reported absolute shielding constants obtained indirectly from NSR constants are in disagreement with the values determined in this work. As already pointed out in earlier studies,[3,10–12,45,59] the indirect determination of absolute shielding constants from NSR tensors leads to inaccurate results due to the missing relativistic corrections to the shielding
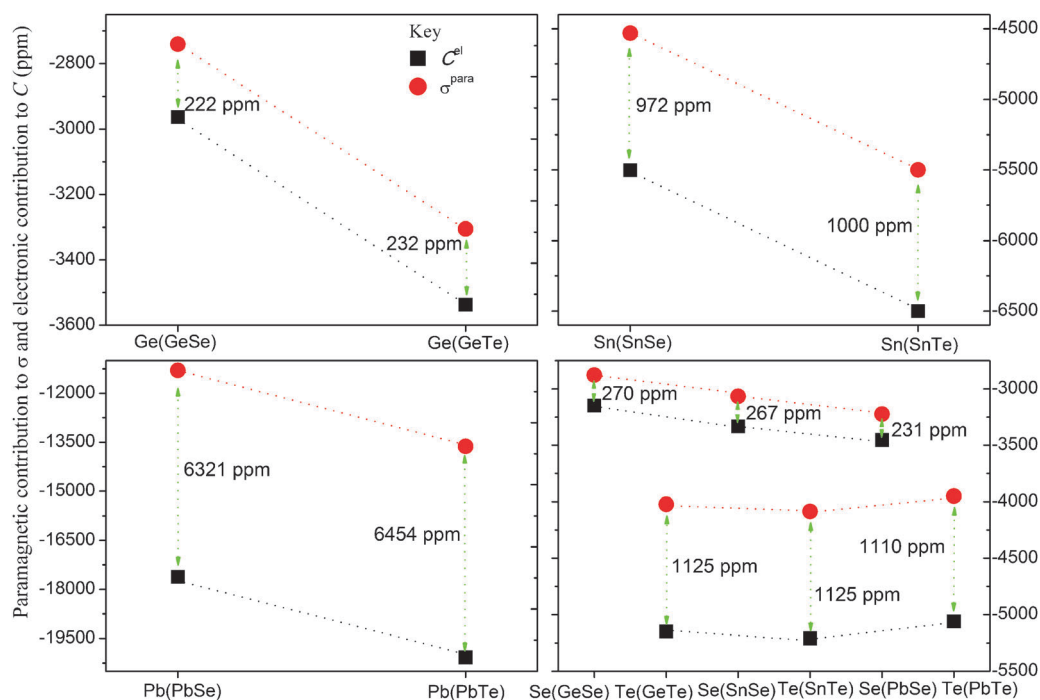

Fig. 1 Comparison of the paramagnetic contribution to the absolute shielding constants ($\sigma^{para,iso}$, the circles) and the electronic contribution to the NSR constants ($C^{el,iso}$, the squares) of XSe and XTe (X = Ge, Sn and Pb) molecules: calculated using DKS/BP86/cv4z. The corresponding values for Si in SiSe and SiTe are both 16 ppm, whereas for Se in SiSe is 271 ppm and for Te in SiTe is 1125 ppm.

3118 | Phys. Chem. Chem. Phys., 2016, 18, 3112–3123

This journal is © the Owner Societies 2016

Table 7 Relativistic corrections, estimated electron correlation effects and final calculated and best estimated values for the absolute shielding constants (σ, in ppm) of nuclei in XSe and XTe (X = Si, Ge, Sn and Pb) molecules together with the previously reported results derived from NSR constants

		Δ(correl)[a]	$\Delta\sigma$(rel 1)[b]	$\Delta\sigma$(rel 2)[c]	CCSD(T)[d]	Total 1[e]	Total 2[f]	Previous	Best estimate[k]
SiSe	Si	195.3	−9.0	−7.2	−56.9	−65.9	−64.1	−106[g]	−65 ± 5
	Se	79.3	184.1	189.7	608.5	792.6	798.2	789[g]	790 ± 10
SiTe	Si	310.4	−59.4	−50.2	−218.9	−278.3	−269.1	−324[g]	−270 ± 16
	Te	305.8	817.7	855.5	1423.8	2241.5	2279.3	2229[g]	2200 ± 123
GeSe	Ge	547.5	−31.4	−35.6	407.3	375.9	371.7	472[h]	380 ± 25
	Se	340.3	146.1	155.7	389.8	535.9	545.5	612[h]	540 ± 38
GeTe	Ge	795.6	−218.5	−221.1	63.5	−155.0	−157.6	−24[h]	−150 ± 16
	Te	717.7	781.5	845.7	1166.2	1947.7	2011.9	2058[h]	1900 ± 105
SnSe	Sn	825.5	−189.4	−244.0	1328.9	1139.5	1084.9	1291[i]	1150 ± 57
	Se	228.4	95.9	119.4	252.3	348.2	371.7	10[i]	360 ± 18
SnTe	Sn	1079.9	−644.4	−723.5	966.4	322.0	242.9	940[i]	330 ± 15
	Te	423.6	815.3	912.3	930.7	1746.0	1843	1753[i]	1700 ± 95
PbSe	Pb	1585.0	−3599.9	−4618.4	3876.7	276.8	−741.7	4712[j]	—
	Se	263.6	19.3	−6.5	−196.9	−177.6	−203.4	−130[j]	−185 ± 10
PbTe	Pb	1894.1	−5076.3	−6052.1	3392.0	−1684.3	−2660.1	3684[j]	−2000 ± 280
	Te	417.3	1033.7	1073.5	828.8	1862.5	1902.3	1705[j]	1800 ± 80

[a] Δ(correl) is an estimated electron correlation effect [CCSD(T)-HF] (see Table 5). [b] $\Delta\sigma$(rel 1) is the difference between DKS and NR results using BP86/cv4z (see Table 5). [c] $\Delta\sigma$(rel 2) is the difference between DKS and NR results using B3LYP/cv4z (see Table 5). [d] unc-ANO-RCC (unc-DZP-DKH for PbTe) basis sets (see Table 5). [e] Total 1 is the sum of $\Delta\sigma$(rel 1) and the CCSD(T) calculated values. [f] Total 2 is the sum of $\Delta\sigma$(rel 2) and the CCSD(T) calculated values. [g] Taken from ref. 27. [h] Taken from ref. 28. [i] Taken from ref. 29. [j] Taken from ref. 30. [k] Error bars are estimated based on calculations performed using different functionals.

tensors (see Tables 5 and 7). The difference is most pronounced for the heavy nuclei, see for instance σ(Pb) in Table 7 and Table S1 of the ESI.† In addition, the diamagnetic contribution used in ref. 27–30 are not accurate enough to estimate the absolute shielding constants. For example, σ^{dia}(Sn) in SnSe in ref. 29 is 6203 ppm, whereas 5236.8 ppm at the DKS/BP86/cv4z level in this work (see Table 6). Test calculations using DKS/BP86/cv4z for the free Sn atom gives a $\sigma^{dia,FA}$(Sn) of 5154.2 ppm. Adding the nuclear contribution $C^{nuc\,5}$ of 83.4 ppm ($\sigma^{dia,FA} + C^{nuc}$) gives 5236.8 ppm, which is in good agreement with the one obtained from direct shielding calculations. In ref. 30, a calculated value of 20 688 ppm was used for σ^{dia}(Pb), which is twice greater than that obtained in this work (10527.0 ppm). Similar test calculations for the free Pb atom give 10431.8 ppm, which becomes 10528.7 ppm together with C^{nuc} (86.9 ppm). Taylor et al.[60] also reported 9950 ppm for σ^{dia}(Pb) and 5311 ppm for σ^{dia}(Te) in $[PbTe_6H_6]^{4-}$ and $[TePb_6F_{18}]^{8-}$ calculated using SO-ZORA/BP86/TZ2P. The CCSD(T)/unc-DZP-DKH calculated values for σ^{dia}(Pb) in this study are 10193.3 ppm in PbSe and 10248.4 ppm in PbTe.

In some molecules there appears to be good agreement between the results calculated in this work and previously estimated values (see Table 7). This is mainly due to error cancellations between σ^{dia} and σ^{para} as there are errors in σ^{dia} used in the earlier studies due to method inaccuracies and the missing relativistic corrections from σ^{para} determined from the experimental C^{el}. For example, in Table 6 it is shown that σ^{para}(Sn) in SnSe determined from the experimental C^{el} is −4912 ppm, whereas σ^{para}(Sn) calculated using DKS/BP86 is −4531.6 ppm ($\Delta\sigma^{para}$ of −380.4 ppm), and σ^{dia}(Sn) used in ref. 29 is 6203 ppm and that obtained in this work is 5236.8 ppm ($\Delta\sigma^{dia}$ of 966.2 ppm), causing a net error cancellation of the two contributions. Considering the levels of calculations used, the final absolute shielding constants of all nuclei reported in this study should be accurate. Based on the results obtained from

different functionals and basis sets, accuracy ranges are also estimated for all the studied nuclei (see Table 7).

3.3. NMR shielding spans

Calculated shielding spans are presented in Table 8, Tables S1 and S2 of the ESI.† The relativistic effects on the shielding spans increase as the nuclei become heavier, compare for example $\Delta\Omega$(rel1) of Ge, Sn and Pb in the corresponding selenide molecules. Relativistic effects are the largest contributions to the span for the lead nuclei in both PbSe and PbTe. For instance, it contributes 18% to the total DKS/BP86 calculated Ω(Ge) in GeTe, 34% to Ω(Sn) in SnTe and 68% to Ω(Pb) in PbTe. The relativistic effects obtained from the two functionals show the largest difference for the span of lead in PbSe and PbTe (11% and 10%, respectively). The effect of the heavy atoms on light atoms (HALA) is another interesting observation from the table. For example, tellurium affects stronger than selenium when we compare the germanium molecules; Ω(Ge) in GeSe calculated using DKS/BP86 is 4477 ppm, while that in GeTe is 5533 ppm. The same is also true for the span of Te when comparing GeTe, SnTe and PbTe, of which lead causes the strongest HALA effect (a difference of 932 ppm between the relativistic correction for the span of Te in SnTe and PbTe at the DKS/BP86/cv4z level).

With the exception of PbSe and PbTe, the shielding spans obtained using the SO-ZORA and DKS methods do not show considerable differences (the maximum difference is 10% for Ω(Sn) in SnTe). SO-ZORA/BP86 underestimates Ω(Pb) by 20% in PbSe and by 27% in PbTe compared to DKS/BP86. In Table 6, the shielding spans determined from the calculated NSR constants and those derived from direct absolute shielding constant calculations are reported. The results show that in the non-relativistic domain, the spans are in perfect agreement with each other. However, there are considerable differences between those obtained in the four-component relativistic calculations.

Table 8 Comparison of the calculated shielding spans (Ω, in ppm) of nuclei in XSe and XTe (X = Si, Ge, Sn and Pb) molecules at different computational levels, relativistic corrections, the final total shielding spans and the previously reported results determined from NSR constants

| | | NR | | SO-ZORA | | DKS | | $\Delta\Omega$(rel 1)[c] | $\Delta\Omega$(rel 2)[d] | CCSD(T)[e] | Total 1[f] | Total 2[g] | Previous |
		BP86[a]	B3LYP[a]	BP86[b]	B3LYP[b]	BP86[a]	B3LYP[a]						
SiSe	Si	1536	1588	1574	1633	1605	1655	69	67	1409	1478	1476	1518[h]
	Se	4064	4083	4286	4280	4284	4294	220	211	3597	3817	3808	3764[h]
SiTe	Si	1797	1886	1918	2031	2005	2083	208	197	1655	1863	1852	1845[h]
	Te	6583	6668	7526	7478	7401	7428	818	760	5917	6735	6677	6505[h]
GeSe	Ge	3938	4043	4358	4504	4477	4594	539	551	3536	4075	4087	3768[i]
	Se	4421	4513	4739	4818	4751	4831	330	318	3928	4258	4246	4028[i]
GeTe	Ge	4510	4692	5228	5520	5533	5732	1023	1040	4055	5078	5095	4514[i]
	Te	7000	7194	8076	8125	7968	8076	968	882	6306	7274	7188	6760[i]
SnSe	Sn	6280	6441	8221	8627	8680	8960	2400	2519	5643	8043	8162	7163[j]
	Se	4647	4742	5163	5256	5198	5264	551	522	4138	4689	4660	4672[j]
SnTe	Sn	7036	7285	9693	10 406	10 654	11 076	3618	3791	6129	9747	9920	7604[j]
	Te	7158	7328	8424	8433	8335	8369	1177	1041	6708	7885	7749	7049[j]
PbSe	Pb	10 705	10 961	26 385	29 767	31 532	34 109	20 827	23 148	9092	29 919	32 240	23 765[k]
	Se	4770	4872	5868	6092	6173	6339	1403	1467	4705	6108	6172	5143[k]
PbTe	Pb	11 900	12 280	29 639	34 092	37 612	40 480	25 712	28 200	10 014	35 726	38 214	25 306[k]
	Te	7266	7434	9059	9189	9375	9482	2109	2048	6818	8927	8866	7172[k]

[a] Using cv4z basis sets (all using GIAO, except B3LYP where CGO was used). [b] Using ZORA optimized all-electron QZ4P basis sets. [c] $\Delta\Omega$(rel 1) is the difference between DKS and NR results using BP86/cv4z (relativistic corrections). [d] $\Delta\Omega$(rel 2) is the difference between DKS and NR results using B3LYP/cv4z (relativistic corrections). [e] unc-ANO-RCC (unc-DZP-DKH for PbTe) basis sets. [f] Total 1 is the sum of the CCSD(T) results and $\Delta\Omega$(rel 1) from BP86/cv4z, absolute values. [g] Total 2 is the sum of the CCSD(T) results and $\Delta\Omega$(rel 2) from B3LYP/cv4z, absolute values. [h] Taken from ref. 27. [i] Taken from ref. 28. [j] Taken from ref. 29. [k] Taken from ref. 30.

For instance, the NR/BP86 results of Ω(Sn) in SnSe are 6279.6 ppm and −6271.0 ppm, for the value obtained from the direct calculation of the shielding constant and that determined from the calculated NSR constant, respectively. The values obtained from the DKS/BP86 calculations for the same nucleus are 8695.6 ppm and −8130.2 ppm, respectively (see Table 6). Such differences are huge for Ω(Pb) in PbSe and PbTe, indicating that using the equation relating the shielding span and NSR constant (eqn (2)) leads to unrecoverable errors for heavy atoms where spin–orbit coupling is prominent. The correlation diagram between the span obtained from these two approaches is shown in Fig. 2. The correlations shows that the error becomes larger as the nuclei become heavier, see for instance the plot for Se in GeSe and in PbSe where the difference is smaller compared to the other nuclei, whereas it is large when we compare Ge, Sn and Pb.

The previously reported shielding spans collected in Table 8 are determined from the experimental NSR constants.[28–30] The equation relating the span and NSR tensors (eqn (2)) works perfectly in the non-relativistic and scalar relativistic domains, whereas for very heavy nuclei, the relation breaks down due to the considerable spin–orbit coupling. We also see these effects in Table 8 where the non-relativistic spans are in relatively good agreement with those derived from the experimental NSR constants for the light atoms. For instance, the NR/BP86 values for Ge in GeTe is 4510 ppm and the previously determined value is 4514 ppm. Also for Te in PbTe, the NR/BP86 value is 7266 ppm which is in fair agreement with the previously reported value of 7172 ppm (see Table 8). However, the differences become large as the nuclei become heavier. For instance, the NR/BP86 calculated value of Ω(Pb) in PbTe is 11 900 ppm, whereas that derived from the experimental NSR constant is 25 306 ppm and the DKS/BP86 result is 37 612 ppm. This difference is mainly due to the large spin–orbit coupling in PbTe.

In Table S1 of the ESI,† a comparison of the scalar and SO contributions to the span of all nuclei are presented. In the NR theory, the span derived from the perpendicular and parallel components of the shielding tensors and those derived from the electronic contribution to the calculated NSR constants are identical. This is in line with our expectation since eqn (2) does not consider relativistic effects. However, surprisingly, the values calculated in the presence of only scalar relativistic effects are also similar, indicating that eqn (2) is also valid in the absence of SO effects. The situation is completely different when SO effects are included, making eqn (2) invalid (see Ω and $C_\perp^{iso}$ of all nuclei calculated using the different methods in Table 6 and Table S1 of the ESI†). For instance, Ω and $C_\perp^{iso}$ of Pb in PbTe calculated using NR/BP86 are 11900.0 and −11889.4 ppm, and those using SC/BP86 are 16640.1 ppm and −16618.0 ppm, whereas those calculated using DKS/BP86 are 37812.2 ppm and −29940.5 ppm, respectively. These analyses indicate that the previously estimated shielding spans from the experimental NSR ($C_\perp$) constants do not represent the nuclei studied (especially the heavy ones) due to the missing relativistic corrections. This can be explained using the modified version of eqn (2) by including the corresponding relativistic corrections:

$$\Omega_K \approx \left| \left(\frac{10^9 m_p}{2 m_e g_K B_r}\right) C_{K,\perp} + \Delta\sigma_{K,\perp}^{para,rel} - \Delta\sigma_{K,\parallel}^{para,rel} - \left(\frac{10^9 m_p}{2 m_e g_K B_r}\right) C_{K,\perp}^{el,rel} \right| \quad (3)$$

where the superscript "rel" indicates the relativistic contribution to the corresponding tensor. When all the relativistic corrections are removed, eqn (3) reduces to eqn (2). Moreover, the net relativistic correction of the span becomes large when $\Delta\sigma_{K,\perp}^{para,rel}$ is dominant compared to the other contributions. For instance, $\Delta\sigma_{K,\perp}^{para,rel}$ and $\Delta\sigma_{K,\parallel}^{para,rel}$ for Ge in GeSe are −231.3 ppm and 312.8 ppm,
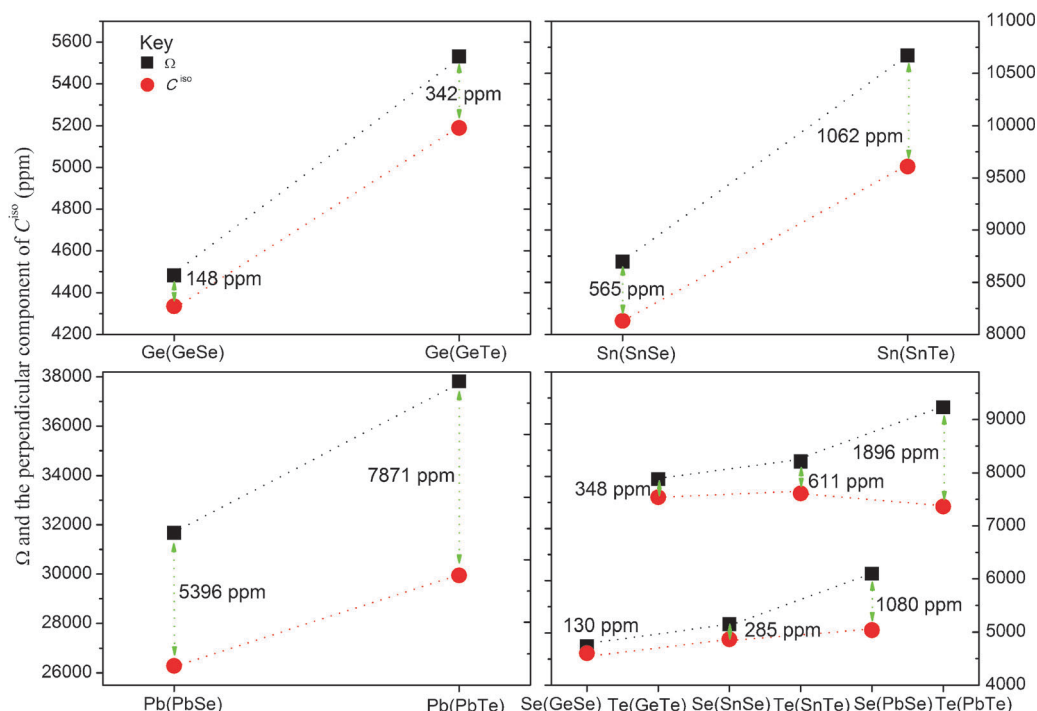
3120 | Phys. Chem. Chem. Phys., 2016, 18, 3112–3123

This journal is © the Owner Societies 2016

Fig. 2 Comparison of the shielding spans (Ω, the squares) and the perpendicular component of the NSR constants ($C_\perp^{iso}$, the circles) of XSe and XTe (X = Ge, Sn and Pb) molecules: calculated using DKS/BP86/cv4z. The corresponding value for Si in SiSe is 43 ppm, in SiTe is 111 ppm, whereas for Se in SiSe is 74 ppm and for Te in SiTe is 250 ppm.

respectively; whereas for Pb in PbTe they are −14216.7 ppm and 11692.9 ppm, respectively, causing a huge relativistic correction for the latter nucleus (see Table S1 of the ESI†).

The final shielding spans are determined by adding $\Delta\Omega$(rel), the difference between the DKS and NR results, to the accurate non-relativistic CCSD(T) results. Unlike the absolute shielding constants, the final results for the spans using the two functionals do not show considerable differences for most of the molecules, with the exception of Ω(Pb) in PbSe and PbTe which show a very large difference in the results obtained with the two functionals. There is good agreement between the calculated spans and those derived from the experimental NSR constants for the light atoms, whereas the agreement deteriorates as the atoms become heavier. For example, the differences between the final calculated and the experimental results for Ω(Si) and Ω(Se) in SiSe are only 2.6% and 1.4%, respectively; whereas the errors for Ω(Pb) and Ω(Te) in PbTe are 41% and 24%, respectively. Considering the levels of the calculations and the shortcomings of eqn (2), the final shielding spans presented in Table 8 should be accurate.

4. Conclusions

In this contribution, the nuclear spin-rotation and absolute shielding tensors of all nuclei in the XSe and XTe (X = Si, Ge, Sn and Pb) molecules, calculated at the non-relativistic (CCSD(T) and DFT) and four-component relativistic DFT levels of theory, are presented. The final calculated results are obtained by

adding the difference between DKS and NR results obtained using either BP86/cv4z or B3LYP/cv4z, Δ(rel), to the non-relativistic CCSD(T) results. The electron correlation effects are more reliably described by coupled-cluster methods than by DFT. Hence, this scheme is used to account for the electron correlation and relativistic effects, giving NSR constants in quite good agreement with the corresponding experimental values.

The relativistic effects on the shielding constants are large compared to the effects on the nuclear spin-rotation constants and shielding spans. The final absolute shielding constants obtained by adding the CCSD(T) calculated results to the $\Delta\sigma$(rel) values obtained from BP86 and B3LYP are in good agreement with each other, showing small effects of the functional used to determine $\Delta\sigma$(rel). There is good agreement between the calculated spans and those derived from experiment for the light atoms, whereas the agreement deteriorates as the atoms become heavier. In addition, the relativistic effects in Ω of the light atoms is small, whereas it becomes huge as the atoms become heavier, see Table 6. For most of the molecules studied, including relativistic effects in the calculations leads to a very significant change of the magnetic properties studied. The difference between the electronic contribution to the spin-rotation constant and the paramagnetic contribution to the shielding shows a periodic trend (see Fig. 1). Overall, the shielding constants and spans of all nuclei reported in this study should be more accurate than the previously reported values determined from the experimental NSR constants due to the lack of relativistic corrections when employing eqn (1) and (2). Even though the scheme used in this study is an immediate

This journal is © the Owner Societies 2016

Phys. Chem. Chem. Phys., 2016, **18**, 3112–3123 | **3121**

remedy for these kinds of calculations, the study points to the need for relativistic coupled-cluster methods for the calculation of magnetic properties.

Acknowledgements

References

1 I. A. Aucar, S. S. Gómez, M. C. Ruiz de Azúa and C. G. Giribet, *J. Chem. Phys.*, 2012, **136**, 204119.

2 I. A. Aucar, S. S. Gómez, J. I. Melo, C. C. Giribet and M. C. Ruiz de Azúa, *J. Chem. Phys.*, 2013, **138**, 134107.

3 E. Malkin, S. Komorovsky, M. Repisky, T. B. Demissie and K. Ruud, *J. Phys. Chem. Lett.*, 2013, **4**, 459–463.

4 N. F. Ramsey, *Phys. Rev.*, 1950, **78**, 699–703.

5 W. H. Flygare and J. Goodisman, *J. Chem. Phys.*, 1968, **49**, 3122–3125.

6 W. H. Flygare, *J. Chem. Phys.*, 1964, **41**, 793–800.

7 W. H. Flygare, *Chem. Rev.*, 1974, **74**, 653–687.

8 Y. Xiao and W. Liu, *J. Chem. Phys.*, 2013, **138**, 134104.

9 Y. Xiao and W. Liu, *J. Chem. Phys.*, 2013, **139**, 034113.

10 K. Ruud, T. B. Demissie and M. Jaszuński, *J. Chem. Phys.*, 2014, **140**, 194308.

11 M. Jaszuński, T. B. Demissie and K. Ruud, *J. Phys. Chem. A*, 2014, **118**, 9588–9595.

12 T. B. Demissie, M. Jaszuński, E. Malkin, S. Komorovský and K. Ruud, *Mol. Phys.*, 2015, **113**, 1576–1584.

13 A. M. Teale, O. B. Lutnæs, T. Helgaker, D. J. Tozer and J. Gauss, *J. Chem. Phys.*, 2013, **138**, 024111.

14 T. Helgaker, J. Gauss, G. Cazzoli and C. Puzzarini, *J. Chem. Phys.*, 2013, **139**, 244308.

15 C. Puzzarini, G. Cazzoli, M. E. Harding, J. Vázquez and J. Gauss, *J. Chem. Phys.*, 2009, **131**, 234304.

16 T. B. Demissie, M. Jaszuński, S. Komorovsky, M. Repisky and K. Ruud, *J. Chem. Phys.*, 2015, **143**, 164311.

17 P. Pyykkö, *Annu. Rev. Phys. Chem.*, 2012, **63**, 45–64.

18 U. Edlund, T. Lejon, P. Pyykkö, T. K. Venkatachalam and E. Buncel, *J. Am. Chem. Soc.*, 1987, **109**, 5982–5985.

19 Relativistic Spectroscopy DFT program of authors S. Komorovsky, M. Repisky, V. G. Malkin, O. L. Malkina, M. Kaupp, K. Ruud, with contributions from R. Bast, U. Ekström, M. Kadek, S. Knecht, I. Malkin Ondik, E. Malkin, ReSpect, version 3.3.0, 2014, see www.respectprogram.org.

20 DIRAC, a relativistic *ab initio* electronic structure program, Release DIRAC13 (2013), written by L. Visscher, H. J. Aa. Jensen, R. Bast, and T. Saue, with contributions from V. Bakken, K. G. Dyall, S. Dubillard, U. Ekström, E. Eliav, T. Enevoldsen, E. Faßhauer, T. Fleig, O. Fossgaard, A. S. P. Gomes, T. Helgaker, J. K. Lærdahl, Y. S. Lee, J. Henriksson, M. Iliaš, Ch. R. Jacob, S. Knecht, S. Komorovský, O. Kullie, C. V. Larsen, H. S. Nataraj, P. Norman, G. Olejniczak, J. Olsen, Y. C. Park, J. K. Pedersen, M. Pernpointner, K. Ruud, P. Sałek, B. Schimmelpfennig, J. Sikkema, A. J. Thorvaldsen, J. Thyssen, J. van Stralen, S. Villaume, O. Visser, T. Winther and S. Yamamoto, see http://www.diracprogram.org.

21 E. J. Baerends, J. Autschbach, A. Berces, F. M. Bickelhaupt, C. Bo, P. M. Boerrigter, L. Cavallo, D. P. Chong, L. Deng, R. M. Dickson, D. E. Ellis, M. van Faassen, L. Fischer, T. H. Fan, C. Fonseca Guerra, S. J. A. van Gisbergen, J. A. Groeneveld, O. V. Gritsenko, M. Gruning, F. E. Harris, P. van den Hoek, C. R. Jacob, H. Jacobsen, L. Jensen, G. van Kessel, F. Kootstra, E. van Lenthe, D. A. McCormack, A. Michalak, J. Neugebauer, V. P. Osinga, S. Patchkovskii, P. H. T. Philipsen, D. Post, C. C. Pye, W. Ravenek, P. Ros, P. R. T. Schipper, G. Schreckenbach, J. G. Snijders, M. Sola, M. Swart, D. Swerhone, G. teVelde, P. Vernooijs, L. Versluis, L. Visscher, O. Visser, F. Wang, T. A. Wesolowski, E. van Wezenbeek, G. Wiesenekker, S. Wolff, T. Woo, A. Yakovlev and T. Ziegler, *ADF2014.01, SCM*, Theoretical Chemistry, Vrije Universiteit, Amsterdam, The Netherlands, 2014, http://www.scm.com.

22 M. Jaszuński, M. Repisky, T. B. Demissie, S. Komorovsky, E. Malkin, K. Ruud, P. Garbacz, K. Jackowski and W. Makulski, *J. Chem. Phys.*, 2013, **139**, 234302.

23 S. Komorovsky, M. Repisky, E. Malkin, K. Ruud and J. Gauss, *J. Chem. Phys.*, 2015, **142**, 091102.

24 K. Hummer, A. Gruneis and G. Kresse, *Phys. Rev. B: Condens. Matter Mater. Phys.*, 2007, **75**, 195211.

25 D. Yu, J. Wu, Q. Gu and H. Park, *J. Am. Chem. Soc.*, 2006, **128**, 8148–8149.

26 X. Sun, B. Yu, G. Ng and M. Meyyappan, *J. Phys. Chem. C*, 2007, **111**, 2421–2425.

27 B. M. Giuliano, L. Bizzocchi and J.-U. Grabow, *J. Mol. Spectrosc.*, 2008, **251**, 261–267.

28 B. M. Giuliano, L. Bizzocchi, R. Sanchez, P. Villanueva, V. Cortijo, M. E. Sanz and J.-U. Grabow, *J. Chem. Phys.*, 2011, **135**, 084303.

29 L. Bizzocchi, B. M. Giuliano, M. Hess and J.-U. Grabow, *J. Chem. Phys.*, 2007, **126**, 114305.

30 B. M. Giuliano, L. Bizzocchi, S. Cooke, D. Banser, M. Hess, J. Fritzschec and J.-U. Grabow, *Phys. Chem. Chem. Phys.*, 2008, **10**, 2078–2088.

31 J. Gauss and J. F. Stanton, *J. Chem. Phys.*, 1995, **102**, 251–253.

32 J. Gauss and J. F. Stanton, *J. Chem. Phys.*, 1996, **104**, 2574–2583.

33 CFOUR, a quantum chemical program package written by J. F. Stanton, J. Gauss, M. E. Harding, P. G. Szalay with contributions from A. A. Auer, R. J. Bartlett, U. Benedikt, C. Berger, D. E. Bernholdt, J. Bomble, L. Cheng, O. Christiansen, M. Heckert, O. Heun, C. Huber, T.-C. Jagau, D. Jonsson, J. Jusélius, K. Klein, W. J. Lauderdale, D. A. Matthews, T. Metzroth, L. A. Mück, D. P. O'Neill, D. R. Price, E. Prochnow, C. Puzzarini, K. Ruud, F. Schiffmann, W. Schwalbach, C. Simmons, S. Stopkowicz, A. Tajti, J. Vázquez, F. Wang,

J. D. Watts and the integral packages MOLECULE (J. Almlöf and P. R. Taylor), PROPS (P. R. Taylor), ABACUS (T. Helgaker, H. J. Aa. Jensen, P. Jørgensen and J. Olsen), and ECP routines by A. V. Mitin and C. van Wüllen. For the current version, see http://www.cfour.de.

34 G. G. Camiletti, A. Canal Neto, F. E. Jorge and S. F. Machado, *THEOCHEM*, 2009, **910**, 122–125.

35 P. J. P. de Oliveira, C. L. Barros, F. E. Jorge, A. Canal Neto and M. Campos, *THEOCHEM*, 2010, **948**, 43–46.

36 A. Canal Neto and F. E. Jorge, *Chem. Phys. Lett.*, 2013, **582**, 158–162.

37 B. O. Roos, R. Lindh, P.-Å. Malmqvist, V. Veryazov and P.-O. Widmark, *J. Phys. Chem. A*, 2004, **108**, 2851–2858.

38 A. D. Becke, *Phys. Rev. A: At., Mol., Opt. Phys.*, 1988, **38**, 3098–3100.

39 J. P. Perdew, *Phys. Rev. B: Condens. Matter Mater. Phys.*, 1986, **33**, 8822–8824, erratum, *ibid.* 1986, **34**, 7406.

40 A. D. Becke, *J. Chem. Phys.*, 1993, **98**, 5648–5652.

41 C. Lee, W. Yang and R. G. Parr, *Phys. Rev. B: Condens. Matter Mater. Phys.*, 1988, **37**, 785–789.

42 P. J. Stephens, F. J. Devlin, C. F. Chabalowski and M. J. Frisch, *J. Phys. Chem.*, 1994, **98**, 11623–11627.

43 S. Komorovsky, M. Repisky, O. L. Malkina, V. G. Malkin, I. Malkin Ondik and M. Kaupp, *J. Chem. Phys.*, 2008, **128**, 104101.

44 S. Komorovsky, M. Repisky, O. L. Malkina and V. G. Malkin, *J. Chem. Phys.*, 2010, **132**, 154101.

45 S. Komorovsky, M. Repisky, E. Malkin, T. B. Demissie and K. Ruud, *J. Chem. Theory Comput.*, 2015, **11**, 3729–3739.

46 K. G. Dyall, *Theor. Chem. Acc.*, 1998, **99**, 366–371.

47 K. G. Dyall, *Theor. Chem. Acc.*, 2006, **115**, 441–447, basis sets available from the Dirac web site, http://dirac.chem.sdu.dk.

48 K. G. Dyall, *Theor. Chem. Acc.*, 2002, **108**, 335–340, erratum, *ibid.* 2003, **109**, 284.

49 F. London, *J. Phys. Radium*, 1937, **8**, 397–409.

50 K. Wolinski, J. F. Hinton and P. Pulay, *J. Am. Chem. Soc.*, 1990, **112**, 8251–8260.

51 P. Manninen, P. Lantto, J. Vaara and K. Ruud, *J. Chem. Phys.*, 2003, **119**, 2623–2637.

52 J. I. Melo, M. C. Ruiz de Azúa, C. G. Giribet, G. A. Aucar and R. H. Romero, *J. Chem. Phys.*, 2003, **118**, 471.

53 E. van Lenthe, E. J. Baerends and J. G. Snijders, *J. Chem. Phys.*, 1994, **101**, 9783–9792.

54 E. van Lenthe, A. Ehlers and E. J. Baerends, *J. Chem. Phys.*, 1999, **110**, 8943–8953.

55 E. van Lenthe and E. J. Baerends, *J. Comput. Chem.*, 2003, **24**, 1142–1156.

56 E. R. Cohen, T. Cvitaš, J. G. Frey, B. Holmström, K. Kuchitsu, R. Marquardt, I. Mills, F. Pavese, M. Quack, J. Stohner, H. L. Strauss, M. Takami and A. J. Thor, *Quantities, Units and Symbols in Physical Chemistry, IUPAC Green Book, 3rd Edition, 2nd Printing*, IUPAC & RSC Publishing, Cambridge, 2008.

57 S. Grimme, *J. Chem. Phys.*, 2010, **132**, 154104.

58 S. Komorovsky, M. Repisky, T. B. Demissie, E. Malkin and K. Ruud, Understanding the atomic nature of the difference between relativistic spin-rotation and NMR shielding constants of the tin atom, unpublished.

59 S. Komorovsky, M. Repisky, E. Malkin, K. Ruud and J. Gauss, *J. Chem. Phys.*, 2015, **142**, 091102.

60 R. E. Taylor, F. Alkan, D. Koumoulis, M. P. Lake, D. King, C. Dybowski and L. S. Bouchard, *J. Phys. Chem. C*, 2013, **117**(17), 8959–8967.

This journal is © the Owner Societies 2016

Phys. Chem. Chem. Phys., 2016, **18**, 3112–3123 | 3123